The Orchha River: Physically based modeling of bedrock incision by abrasion, plucking and macro abrasion

"Every man has his secret sorrows which the world knows not; and often times
We call a man cold when he is only sad."

— Henry Wadsworth Longfellow

Rajkumar Dongre

The Orchha River in rainy days -Channel incision into bedrock plays an important role in orogenesis by setting the lower boundaries of hillslopes. The longitudinal profiles of bedrock channels constitute a primary component of the relief structure of mountainous drainage basins and thus channel incision limits the elevation of peaks and ridges

---

Keyword: Macroabrasion, Orchha, Knick dominate, bed rock River, Chunks.

Abstract

[1] Many important insights into the dynamic coupling among climate, erosion, and tectonics in mountain areas have derived from several numerical models of the past few decades which include descriptions of bedrock incision. However, many questions regarding incision processes and morphology of bedrock streams still remain unanswered. A more mechanistically based incision model is needed as a component to study landscape evolution. Major bedrock incision processes include (among other mechanisms) abrasion by bed load, plucking, and macro abrasion (a process of fracturing of the bedrock into pluckable sizes mediated by particle impacts).

Mobile: 09301953221, Email: rajkumardongre@gmail.com

The purpose of this paper is to develop a physically based model of bedrock incision that includes all three processes mentioned above. To build the model, we start by developing a theory of abrasion, plucking, and macroabrasion mechanisms. We then incorporate hydrology, the evaluation of boundary shear stress, capacity transport, an entrainment relation for pluckable particles, a routing model linking in-stream sediment and hillslopes, a formulation for alluvial channel coverage, a channel width relation, Hack's law, and Exner equation into the model so that we can simulate the evolution of bedrock channels. The model successfully simulates various features of bed elevation profiles of natural bedrock rivers under a variety of input or boundary conditions. The results also illustrate that knickpoints found in Bedrock Rivers may be autogenic in addition to being driven by base level fall and lithologic changes. This supports the concept that bedrock incision by knickpoint migration may be an integral part of normal incision processes. The model is expected to improve the current understanding of the linkage among physically meaningful input parameters, the physics of incision process, and morphological changes in bedrock streams.

---

1. Introduction

[2] Channel incision into bedrock plays an important role in orogenesis by setting the lower boundaries of hillslopes. The longitudinal profiles of bedrock channels constitute a primary component of the relief structure of mountainous drainage basins and thus channel incision limits the elevation of peaks and ridges [*Whipple and Tucker*, 1999]. Despite the need for physical understanding of various bedrock incision processes that drive landscape evolution, relatively little research has focused on a fully mechanistic or physically based model of incision [e.g., *Sklar and Dietrich*, 2004; *Lamb et al.*, 2008]. In the past few decades, the majority of numerical models of large-scale, landscape evolution have used stream power models [e.g., *Willgoose et al.*, 1991; *Seidl et al.*, 1994; *Tucker and Slingerland*, 1994; *Willett*, 1999] or modified versions that implicitly include the role of sediment load in eroding the channel bed [e.g., *Gasparini et al.*, 2006, 2007]. Such models lump the physics of bedrock incision into very simple laws for the purpose of modeling landscape evolution. Such models are indeed the right place to begin the study of mountain landscape evolution, and they can provide qualitative and partial quantitative insight into the linkages among climate, erosion, and tectonics [e.g., *Whipple and Tucker*, 2002; *Gasparini et al.*, 2007]. In the context of a higher level of analysis inspired by these models themselves, however, it becomes apparent that they lack versatility in that they amalgamate the complicated controls of such basic variables as rainfall rate or flow discharge, channel slope, rock strength, sediment supply, fraction of bedrock exposure, grain size, channel width, dominant incisional mechanisms, and bed roughness into a set of simplified parameters (typically bed slope and drainage area upstream) and exponents. However, *Gasparini et al.* [2007] demonstrated that the traditional stream power law in fact can derive from a more physically based and complicated model by bed load abrasion [e.g., *Sklar and Dietrich*, 2004] despite its simple scaling. Thus the stream power models are somewhat physically based and, to certain extent, can provide us some insights regarding landscape evolution.

[3] *Sklar and Dietrich* [1998, 2004] were among the first (also *Foley* [1980]) to propose a mechanistic model for bedrock wear (abrasion) by saltating bed load. They combined the roles of the tool effect (more tools scraping the bed produce more incision) and the cover effect (the greater the fraction of the bed that is covered with alluvium, the less incision can occur). However, their model considers only the process of abrasion by saltating bed load. In natural

bedrock streams, channel incision can also result from plucking (the direct removal of broken pieces of bedrock from the bed) and macro abrasion (a process of fracturing of the bedrock, confined in the top layer, into pluckable sizes through the collision by wear particles) [*Whipple et al.*, 2000a]. In some bedrock streams, channel incision may combine two or all of these major mechanisms together, while in a bedrock stream with a very hard bedrock type such as some limestones, plucking-macroabrasion processes may even dominate the channel incision process.

[4] In addition to the above three processes, i.e., wear, plucking, and macroabrasion, other bedrock incision processes may include cavitation, dissolution, and abrasion by suspended load [e.g., *Whipple et al.*, 2000a]. *Lamb et al.* [2008] have recently developed a mechanistic model of bedrock incision due to suspended-load abrasion and suggested that bedrock erosion by suspended load could be important in some bedrock streams with steep slopes, small particle sizes, and high sediment supply rates. Here, however, analysis is focused on the three processes of bed load abrasion, plucking, and macroabrasion, simply because we focus on incision processes by bed load.

[5] Generally, the term "abrasion" should refer to the wear induced by one surface sliding with friction over another. In fact, the term "abrasion" traditionally does not seem to even cover the processes of cutting and deformation that comprise the particle impact wear model of *Foley* [1980] or *Bitter* [1963a, 1963b]; rather, it seems strictly reserved for sustained surface-surface contact drag and frictional wear. The geomorphology community now (including our work here) uses the term "abrasion" in a looser way and often uses it interchangeably with the term "wear." It is rather late to preserve the physical fidelity of the term outside the tribology (the science of the mechanisms of friction, lubrication, and wear of interacting surfaces that are in relative motion) literature.

[6] Relatively few studies have been done on observations of plucking-dominated bedrock streams in the past few decades [e.g., *Miller*, 1991; *Tinkler and Parish*, 1998; *Whipple et al.*, 2000a, 2000b; *Dubinski and Wohl*, 2005]. *Miller* [1991] We investigated knickpoint development and channel-bed degradation along several downcutting, plucking-dominated bedrock streams in Abujhmarh, India. We found that knickpoints separated by concave-upward stream segments are more common in plucking-dominated streams rather than abrasion-dominated streams, which are in the same area but associated with a different bedrock type. *Dubinski and Wohl* [2005] were probably the first to conduct an experiment regarding incision processes by plucking using a flume filled with three layers of blocks. They found that a persistent retreating knickpoint with episodic quarrying of blocks at the knickpoint occurred during all the runs. Knickpoints are occasionally found in Bedrock Rivers (both abrasion- and plucking-dominated settings) at locations unrelated to lithology, tributary convergence, or uplift [*Woodford*, 1951].

[7] *Whipple et al.* [2000a] made the intriguing observations that (1) substrate lithology appears to control the dominant erosion process, specifically abrasion versus plucking, and that (2) joint spacing, fractures, and bedding planes have the most direct control on the processes. Although *Whipple et al.* [2000a, 2000b] have applied the concept of stream-power models to plucking-dominated bedrock streams and investigated the significance of the exponent in power laws for slope, these models do not in and of themselves provide direct insight into the physics behind incision processes. Therefore the development of a physically based model of bedrock incision that includes wear, plucking, and macroabrasion should be useful for the understanding of the landscape evolution resulting from these processes.

[8] The purpose of this paper is to develop a physically based model of bedrock incision in the Abujhmarh that includes processes of abrasion by saltating bed load, plucking, and macroabrasion. The goals are to (1) be able to make specific statements about physical mechanisms of bedrock incision and (2) delineate parameters with meaningful dimensions that offer the hope of quantifying the problem based on field and laboratory data. The model and its various input parameters and boundary conditions are discussed. Here, we especially aim to test the incision model developed where both bed load abrasion and plucking mechanisms are considered in the incision processes.

2. Model Development

[9] This section presents the development of the theoretical model by considering bedrock incision processes by abrasion, plucking, and macroabrasion. Each individual process of incision can also be considered alone by suppressing the other processes. For example, if we would like to adapt the model to investigate a plucking-dominated bedrock channel, we can set the abrasion coefficient to be a very small value so that the abrasion process is not effective. Realistic values of input parameters can help provide guidance as to what incision processes would dominate in any given river. For some bedrock rivers, all processes may be equally important, in which case the three processes interact nonlinearly.

[10] We start from a consideration of abrasion by wear, the tool effect associated with sediment transport, and the cover effect provided by alluvial deposition. We then develop a theoretical model of incision mechanisms by plucking and macroabrasion to add into the pure bed load abrasion process. We incorporate hydrology (e.g., rainfall events), the concept of boundary shear stress, the concept of capacity transport, an entrainment relation of pluckable particles, a routing model linking in-stream sediment and the adjacent hillslope, a channel width relation, Hack's law, and the Exner equation into the model so that we can simulate the evolution of the long profile of bedrock channels.

[11] Note that here only vertical incision is considered and lateral incision is omitted for simplicity. Several studies [e.g., *Stark and Stark*, 2001; *Turowski et al.*, 2008; *Wobus et al.*, 2008] have been done regarding lateral incision processes. Our model has a fixed channel geometry, which excludes temporal width variation from the lateral erosion dynamics. However, this can be incorporated into a subsequent version in the future.

2.1. Abrasion Process Driven by Collision

[12] The abrasion or wear process presented here derives from the original work of *Sklar and Dietrich* [1998, 2004], but with some modifications. Wear or abrasion is the process by which bedrock is ground to sand or silt. The clasts that do the abrasion are assumed to have a characteristic size D_a. Let x denote down-channel distance and let $q(x)$ denote the volume transport rate of sediment in the stream per unit width during a storm event. Let the fraction of this load that consists of particles coarse enough to do the wear be α [e.g., *Whipple and Tucker*, 2002]. The volume transport rate per unit width q_a of sediment coarse enough to abrade the bedrock is then given as

$$q_a = \alpha q \tag{1}$$

For simplicity, α might be set equal to the fraction of the load that is gravel or coarser yet capable of moving during the floods of interest. Consider the case of saltating bed load particles. Let ζ denote the volume rate at which saltating wear particles bounce off the bed per unit bed area

and L_s denote the characteristic saltation length of wear particles. It follows from simple continuity that

$$q_a = \zeta L_s \tag{2}$$

[13] The mean number of bed strikes by wear particles per unit bed area per unit time is equal to ζ / V_a, where V_a denotes the volume of a wear particle. It is assumed that with each collision a fraction r of the particle volume is ground off the bed and a commensurate but not necessarily equal amount is ground off the wear particle. The rate of vertical bed incision *Ea* due to abrasion is then given as (number of strikes per unit bed area) × (volume removed per unit strike) or

$$E_a = \frac{\zeta}{V_a} r V_a \tag{3}$$

Reducing (3) with (2), it is found that

$$E_a = \beta q_a \tag{4a}$$

$$\beta = \frac{r}{L_s} \tag{4b}$$

[14] Here the parameter β has the dimensions [1/L] and is assumed to be a constant. It has exactly the same status as the abrasion coefficients used to study downstream fining by abrasion in rivers [e.g., *Parker*, 1991]. Comparing with *Sklar and Dietrich* [2004] formulation, the abrasion coefficient can be defined physically as

$$\beta = \frac{\rho_s W_{si}^2 Y}{k_v \sigma_T^2 L_s} \tag{5}$$

where ρ_s is rock density (M/L^3); *wsi* is vertical sediment impact velocity (L/T); *Y* is Young's modulus of elasticity of rock (M/L/T^2), which could be assumed as a constant value of 5×10^4 MPa as suggested by *Sklar and Dietrich* [2004], although the value can slightly vary with rock type (J. Johnson, personal communication, 2006); k_v is dimensionless rock resistance constant ($\sim 1 \times 10^6$); and σ_T is rock tensile strength (M/L/T^2). Note that there was a typographical error in the work of *Sklar and Dietrich* [2004]regarding the dimensionless value of k_v, which is not 1.0×10^{12} as stated in their original work . By scaling analysis, a reasonable range of the abrasion coefficient is in the order of 10^{-6} m^{-1} (for hard rocks such as quartzite or andesite) to 10^{-4} m^{-1} (for weak rocks such as weathered sandstone).

[15] The original work by *Sklar and Dietrich* [2004] stated that only the case where the bedrock surface is planar is considered, mostly because there are derivations of saltation trajectories of grains involved in their model. These derivations are based on the data of grain saltation over alluvial bed from literatures. Our work here is, however, rather different. Since we have simplified the abrasion capability as a single parameter (β), which can be specified as constant, it should be fair to state that our model can be generalized to include the case of no uniform bed topographies (e.g., inner channels, step-pool sequences, or potholes). The scale of feedback between these no uniform bed features and bed lowering has been shown to be important in bedrock incision processes [e.g., *Johnson and Whipple*, 2007; *Finnegan et al.*, 2007; *Johnson*, 2007].

2.2. Cover Factor of Alluvial Deposits

[16] Equation (4a) is valid only to the extent that all wear particles collide with exposed bedrock. If wear particles partially cover the bed, the wear rate should be correspondingly

reduced. This effect can be quantified in terms of the ratio q_a/q_{ac}, where q_{ac} denotes the capacity transport rate of particles in the size range that do the abrasion. Let p_0 denote the areal fraction of surface bedrock that is not covered with wear particles. In general p_0 can be expected to approach unity as $q_a/q_{ac} \rightarrow 0$, and approach zero as $q_a/q_{ac} \rightarrow 1$. Various authors, [e.g., *Sklar and Dietrich*, 1998; *Slingerland et al.*, 1997], have proposed the form

$$p_0 = \left(1 - \frac{q_a}{q_{ac}}\right)^{n_0} \tag{6}$$

where n_0 is an exponent (e.g., $n_0 = 1$ indicating the linear relation). *Chatanantavet and Parker* [2008]found that in general the value $n_0 = 1$ seems reasonable for many cases. Equation (4a), the relation for vertical incision due to abrasion, is then modified to

$$E_a = \beta q_a p_0 = \beta_{aq}\left(1 - \frac{q_a}{q_{ac}}\right)^{n_0} \tag{7}$$

Note that equation (7) include both the tool effect (incision increases with increasing q) and the cover effect (incision decreases with increasing q). Note also that E_a drops to zero when αq becomes equal to qac, downstream of which a completely alluvial gravel bed stream is found. It is important to note that equation (7) implicitly assumes that the bed coverage is event-scale. *Turowski et al.* [2007] made the point that the history of sediment flux and transient deposition needs to be considered and they derived a formulation of bed cover based on the negative exponential function of sediment supply to capacity ratio. *Stark et al.* [2009] used a different approach that also takes into account the long-term intermittency of bed load flux and its effect on bed cover. Although the linear relation of bed cover we use here (equation (7)) is simple and does not consider sediment storage and bed load flux intermittency, *Chatanantavet and Parker* [2008] proved that it is generally a reasonable formula for bed cover in a river channel. In fact, they found that long-term antecedent deposition actually promotes the linear relation of bed cover with transport rate by increasing the hydraulic roughness of the bed. In a steep slope channel with high-Froude-number flow, they also found that thick sediment deposits were washed away rapidly and it may either leave some patches of sediment commensurate with supply or expose the bedrock bed entirely.

2.3. Capacity Bed Load Transport Rate of Effective Tools, Boundary Shear Stress, and Hydrology

[17] The parameter q_{ac} can be quantified in terms of standard bed load transport relations. A generalized relation of the form of *Meyer-Peter and Müller* [1948], for example, takes the form

$$q_{ac} = \sqrt{R g D_a D_a}\,\gamma T\left(\frac{\tau_b}{\rho R g D_a} - \tau_c^*\right)^{nT} \tag{8}$$

where g denotes the acceleration of gravity, ρ denotes water density, τ_b denotes bed shear stress, $R = (\rho_s/\rho) - 1$ where ρ_s denotes sediment density, τ_c^* denotes a dimensionless critical Shields number, γT is a dimensionless constant, and nT is a dimensionless exponent. For example, in the implementation of *Fernandez Luque and van Beek* [1976], $\gamma T = 5.7$, $nT = 1.5$, and τ_c^* is between 0.03 and 0.045. The standard formulation for boundary shear stress places it proportional to the square of the flow velocity $U = q_w/H$, where q_w denotes the water discharge per unit width and H denotes flow depth. More precisely,

$$\tau_b = \rho C_f \frac{q_w^2}{H^2} \tag{9}$$

where C_f is a friction coefficient for a completely alluvial bed, which is here assumed to be constant for simplicity. In the case of the characteristically steep slopes of bedrock streams the normal flow approximation, according to which the downstream pull of gravity just balances the resistive force at the bed, should apply, so that the bed shear stress τ_b can be estimated as

$$\tau_b = \rho \mathrm{g} H S \tag{10a}$$

where S denotes the slope of the bedrock river. Between (9) and (10a), it is found that

$$\tau_b = \rho C_f^{1/3} \mathrm{g}^{2/3} q_w^{2/3} S^{2/3} \tag{10b}$$

Now let i denote the precipitation rate, $W(x)$ denote channel width, and $A(x)$ denote the drainage area. Assuming no storage of water in the basin and that flood discharge scales with drainage area, the balance for water flow is

$$q_w W = iA \tag{11}$$

[18] Between (8), (10b), and (11), the capacity bed load transport rate of effective tools for wear is given as

$$q_{ac} = \sqrt{RgD_a} D_a q_{ac}^* \tag{12a}$$

$$q_{ac}^* = \gamma r \left[\frac{C_f^{1/3} i^{2/3} X^{2/3}}{R \mathrm{g}^{1/3} D_a} S^{2/3} - \tau_c^* \right]^{nt} \tag{12b}$$

where

$$X = \frac{A}{W} \tag{12c}$$

Note here that χ has the dimension of length and serves as a surrogate for down-channel distance x in this model.

2.4. Mechanism for the Plucking Processes

[19] Plucking can be conceptualized as follows. There is an "aging layer" just below the surface of the bedrock of thickness L_a in which the bedrock is gradually becoming fractured and loosened over time by (1) stress release within the rock layer, (2) repeated wetting and drying in the case of bedrock with high clay minerals, (3) bioturbation of the surface layer in the case of weakly consolidated mud bedrock, or (4) surface chemical effects. The process of fracturing leads to the formation of chunks that can be plucked and transported out. The process by which an unfractured aging layer of thickness L_a (dimension [L]) becomes fractured to pluckable sizes is governed by an "aging time" T_{pa} (dimension [T]) which loosely corresponds to a half-life for fracturing in the aging layer.

Figure 1. (a) A Photograph of Waterfall on the Orchha River. A schematic bedrock incision by plucking processes. D_p is a characteristic size of pluckable stone and L_a is thickness of aging layer. (b) A surface of pluckable chunks on a plucking-dominated bedrock stream in Orchha River ,Abujhmarh..

[20] This aging layer is capped by a "battering layer" of thickness D_p, where D_p is a characteristic size of pluckable stone (Figure 1a). Within the battering layer the process of fracturing is abetted by wear particles that collide with the surface of the battering layer. Thus the wear particles act to increase the natural frequency of fracturing (macroabrasion) and thus the production of pluckable particles, in addition to grinding away the bedrock to sand or silt (pure abrasion).

[21] For simplicity the model assumes just two sediment sizes, i.e., a size D_a that actually does the abrasion and abets the fracturing and a size D_p ($> D_a$) for the characteristic dimension of a fractured piece of bedrock that can be plucked out and removed. In addition to these two sizes, it is assumed that there is a "wash load" of finer material that is ineffective as an agent of either wear or macroabrasion. For example, the sand and silt might be treated as wash load in regard to bedrock incision, D_a might be a typical gravel size (up to boulder size in some cases), and D_p might be equivalent to a cobble size. The model can presumably be generalized for full grain size distributions.

[22] Within the aging layer it is assumed that the bedrock is gradually broken up into pluckable chunks of characteristic size $D_p$over time. Particles in the aging layer are protected from the bed load transport of wear particles by the battering layer above, so the process is assumed to proceed independently of channel transport. While the basic image here is that of rock fracture, the idea can apply to cracking of clay-mineral-rich bedrock due to repeated wetting and drying and breakup of partially consolidated clay due to bioturbation as well. Let p_{pa}denote the volume fraction of material in the aging layer that has broken up into pluckable chunks. The following relation is derived from the mass conservation law for the time variation of p_{pa}.

$$\frac{\partial p_{pa}}{\partial t} = \frac{1}{T_{pa}}\left(1 - p_{pa}\right) - \frac{IE}{L_a} p_{pa} \tag{13}$$

where t denotes time, I denotes flood intermittency (fraction of time the river is experiencing a flood of sufficient magnitude to render the stream morphologically active), and E denotes the total vertical bedrock incision rate by all processes. The first term on the right-hand side of (13) describes an exponential/logistic breakup over time, where T_{pb} is a parameter with the dimension [T] that is proportional to a "half-life" for the aging layer to break up completely into movable chunks. The term $(1 - p_{pa})$ quantifies the fact that material that has already broken up is no longer available for further breakup. The second term on the right-hand side of (13) describes the rate at which unbroken rock from below is incorporated into the aging layer as the channel incises. The parameter $1/T_{pb}$can be interpreted as the frequency at which fracturing (or an equivalent mechanism) produces a pluckable chunk within the aging layer and is thus probably quantifiable based on field measurements.

[23] Let p_{pb} denote the volume fraction of material in the battering layer that consists of pluckable particles and T_{pb} denote the time constant associated with enhanced breakup due to battering. Within the battering layer, then,

$$\frac{\partial p_{pa}}{\partial t} = \left(\frac{1}{T_{pa}} - \frac{1}{T_{pb}}\right)\left(1 - p_{pb}\right) - \frac{IE}{D_P}\left(P_{pb} - p_{pa}\right) \tag{14}$$

In the second term on the right-hand side of (14), the term $(P_{pb} - p_{pa})$ quantifies the rate at which volume of pluckable particles are lost from the top of the layer (to bed load transport) and gained from the bottom of the layer (from the aging layer) as incision proceeds.

2.5. Mechanism for Macroabrasion Processes

[24] Within the battering layer in Figure 1a, the process of breakup to pluckable sizes is abetted by the collision of wear particles with the bed, a process that has been termed "macroabrasion." The basic assumption of the process for macroabrasion used here is that the more frequently wear particles strike the surface of the battering layer, the higher the rate of production of pluckable particles due to fracturing or related processes. As noted in the description of the mechanism for wear, the number of wear particles that strike the bed per unit time per unit bed area is equal to ζ/V_{ma} where V_{ma} denotes the volume of a wear particle big enough to result in cracking and eventually macroabrasion. Now let A_p denote some measure of the surface area of a pluckable particle (Figure 1b). The number of strikes per unit time on a zone of battering layer surface with area A_p is thus given as $\zeta A_p/V_{ma}$. Assuming a linear relation between the number of strikes per unit time on this area and the frequency at which the area fractures into a pluckable particle, then,

$$\frac{1}{T_{pb}} \sim \zeta \frac{A_p}{V_{ma}} \sim \zeta \frac{D_p^2}{D_{ma}^2} \tag{15}$$

where D_{ma} $(> D_a)$ is the mean characteristic size of the wear particles that effectively do the macro abrasion by hitting the bed and inducing cracks. Now between (2) and (15) it is seen that

$$\zeta \frac{D_p^2}{D_{ma}^3} = \frac{q_a}{L_s} \frac{D_p^2}{D_{ma}^3} = \frac{1}{r} \beta q_a \frac{D_p^2}{D_{ma}^3} \tag{16}$$

The proportionality (15) is converted to equality with the aid of (16) and a parameter ϕ'_{ma}, so that

$$\frac{1}{T_p b} = \frac{\phi'_{ma}}{r} \beta q_a \frac{D_p^2}{D_{ma}^3} = \phi_{ma} \beta q_a \frac{D_p^2}{D_{ma}^3} \tag{17}$$

Here $\phi_{ma}$is a dimensionless parameter characterizing macroabrasion.

2.6. Entrainment Relation and Incision Mechanism in Plucking-Macroabrasion Processes

[25] Pluckable chunks are assumed to have size $D_p > D_a$. these are assumed to be entrained into bed load transport by the flow. Let q_p denote the volume rate of entrainment of pluckable chunks into bed load transport per unit bed area per unit time. (Once a particle is entrained into bed load, it typically undergoes many saltations before it completes one step length.) Standard relations for entrainment into bed load transport have been available since Einstein. Here the form of a relation due to *Tsujimoto* [1999] is used:

$$q_p = \sqrt{R g D_p} q_p^* \tag{18a}$$

where γE is a dimensionless constant, nE is a dimensionless exponent, and τ_{cp}^* is a critical Shields number for entrainment of pluckable grains, which is liable to be somewhat larger than τ_c^*

because the grains in question are liable to have block-like shapes. *Tsujimoto* [1999] suggests the following values: $\gamma E = 0.0199$ and $n_E = 1.5$ as well as $\tau_{cp}^* = 0.045$.

[26] The incision rate due to plucking, E_p, can be given as

$$E_p = q_p p_{pb} p_0 \tag{19}$$

According to (19), incision by plucking cannot occur if the bed is covered with alluvium ($p_0 = 0$), nor can it occur if pluck able chunks are not available in the battering layer ($p_{pb} = 0$). Reducing (19) with (10), (11), and (18), it is found that

$$E_p = \sqrt{R\mathrm{g}D_p}\gamma E \left[\frac{C_f^{1/3}\mathrm{g}^{2/3}\mathrm{i}^{2/3}\chi^{2/3}}{R\mathrm{g}D_p} S^{2/3} - \tau_{cp}^*\right]^{nE} P_{pb} p_0 \tag{20}$$

Once pluckable grains are removed, they should in principle be added to the abrasion-effective load q_a. This is not done here simply because the rate of mass production of sediment from direct incision from the bed is liable to be only a tiny fraction of the production of wear-effective sediment from the hillslopes.

2.7. Linking In-Channel Sediment and Hillslope Material

[27] A routing model is necessary to determine q and thus q_a It is assumed as a first crude assumption here that the local fluvial incision lowers the adjacent hillslope by landslide processes at the same rate. (This assumption can be modified in a more detailed model to include regolith production and hillslope diffusion.) The equation of sediment conservation on a bedrock reach can then be written as

$$\frac{d}{dx}(qW) = qh \tag{21}$$

where qh denotes the volume of sediment per stream length per unit time entering the channel from the hillslopes (either directly or through the intermediary of tributaries) as shown in Figure 2. Note again that a more sophisticated model might later include the development of regolith on hillslopes. Several models can be postulated for qh depending on hillslope dynamics. Here, it is assumed that the watershed consists of easily weathered rocks so that bed lowering by channel incision results in hillslope lowering at the same rate. In this case, we have

$$q_h = E\frac{dA}{dx} \tag{22}$$

As illustrated in Figure 2. Note that in (22), *E* is the total incision rate by all processes. Moreover, this equation serves only as a simple example that must later be generalized to include, e.g., hillslope diffusion, hillslope relaxation due to landslides driven by earthquakes, or saturation in the absence of uplift.

[28] Between (21) and (22) it is found that

$$\frac{d}{dx}(qW) = E\frac{dA}{dx} \tag{23}$$

which relates vertical incision, hillslope materials, and in-stream sediment transport. To obtain a first approximate treatment for the case of deviation from steady state incision, we start from an

empirical relation between channel width and the drainage area upstream [e.g., *Montgomery and Gran*, 2001], defined as

$$W = \alpha_b A^{nb} \tag{24a}$$

or equivalently using (12c)

$$W = \tilde{a}_b \chi^{mb} \tag{24b}$$

$$\breve{a}_b = a_b^{1/(1-n_b)} \tag{24c}$$

$$m_b = \frac{n_b}{1-n_b} \tag{24d}$$

[29] Generally, $\alpha b \sim 0.002$ to 0.088 and $nb \sim 0.3$ to 0.5 where channel width is in meters and drainage area is in square meters [e.g., *Montgomery and Gran*, 2001; *Whipple*, 2004; *Wohl and David*, 2008]. Drainage area *A* can be written as a function of down-channel distance x using an appropriate form of Hack's law [*Hack*, 1957] below:

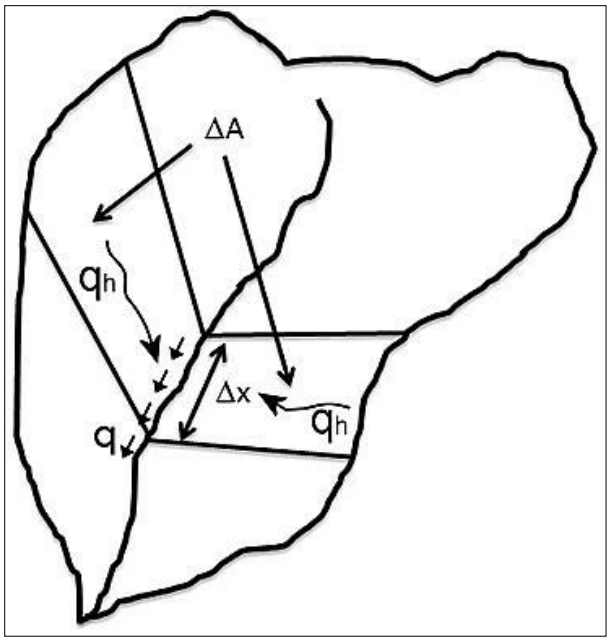

Figure 2. Illustration of a drainage basin showing the source of the sediment delivered from hillslopes as the streambed incises. Δx denotes a segment of down channel distance. ΔA denotes a segment of the drainage area for the distance Δx, qh denotes the volume of sediment per stream length per unit time entering the channel from the hillslopes, and q denotes the total volume sediment transport rate per unit width.

$$A = K_h \chi^{nh} \tag{25}$$

According to *Hack* [1957], when channel length is in meters and drainage area is in square meters, the appropriate values are $K_h \sim 6.7$ and $n_h \sim 1.7$. Often field data, derived from topographic maps, show a deviation from these values. Several studies [e.g., *Stark*, 1991; *Maritan et al.*, 1996; *Rigon et al.*, 1996, 1998] have shown that at least part of the anomalous scaling (e.g., $n_h \neq 1.7$) is the result of a fractal scaling of the mainstream length and its dependence on the resolution of the mapping. They have also argued that the scaling is allometric (self-affine), which may not be applicable when extended over several orders of magnitude (very large basin). Between (23) and (24b), one finds

$$q = \frac{m_b + 1}{\chi^{mb}} \int_0^x E \chi_1^{m_b} d\chi_1 \tag{26}$$

where the total bedrock incision rate E is given as

$$E = E_a + E_p \tag{27}$$

In (26), the in-stream sediment transport derives from total sediment production delivered from the hillslope driven by vertical channel incision, including all incisional processes. Although the model does not specifically describe these hillslope processes, they are usually dominated by landslides (only component captured here) and hillslope diffusion. Here we only consider the case of hillslope response, not the catchment tributary response although the latter can be modified and studied later as a network of channels.

2.8. Exner Equation

[30] If a river is assumed to be morphologically active only intermittently (during floods of interest), the Exner equation (i.e., mass balance statement) for bedrock rivers becomes

$$\left(1 - \lambda_p\right) \frac{\partial \eta}{\partial t} u - IE \tag{28a}$$

where υ is the relative rock uplift rate, λ_p is the porosity of bedrock (perhaps ~0 in many cases), η is elevation of the river bed, and we is the intermittency of large flood events at which the river is morphologically active in regard to incision. Equation (28a) can be viewed as the competition between the relative rock uplift rate and the incision rate, resulting in the rate of change of bed elevation. Uplift is not really continuous, but at geological scale it is treated as such here. In the case of a more general flood hydrograph, the formulation can be generalized to

$$\left(1 - \lambda_p\right) \frac{\partial \eta}{\partial t} u - \sum_{k=1}^{N} I_k E_k \tag{28b}$$

in which I_k is fraction of time the flood flow is in the kth flow range.

2.9. Assembling All Submodels

[31] Here all processes of incision in Bedrock Rivers are considered. From (7), (19), and (26) one finds the total incision as follows:

$$E = E_a + E_p = \left\{ \left[\beta \alpha \left(\frac{m_b + 1}{\chi^{mb}} \int_0^x E \chi_1^{mb} \, d\chi_1 \right) \right] + q_p p_{pb} \right\}$$

$$* \left[1 - \frac{a \left(\frac{m_b + 1}{\chi^{mb}} \int_0^x E \chi_1^{mb} \, d\chi_1 \right)}{q_{ac}} \right]^{n_a} \tag{29}$$

The above equation has two limits of interest. When the abrasion coefficient β approaches zero, or is extremely small (e.g., $\leq 10^{-6}$ m^{-1}), and the term $q_p p_{pb}$ indicating both the availability and transportability of pluckable particles is not similarly small, then plucking becomes the dominant process of incision. When, on the other hand, β is sufficiently large, abrasion dominates plucking.

[32] In order to solve (29), it is useful to introduce a new auxiliary variable

$$\mathrm{B} = \int_0^x E \chi_1^{mb} \, d\chi_1 \tag{30}$$

from which it is found that

$$E = \frac{1}{\chi^{m_b}} \frac{dB}{d\chi} \tag{31}$$

From (29), one then obtains the following first-order ordinary differential equation:

$$\frac{dB}{d\chi} = \{[\beta_a(m_b)] + [\chi^{m_b} q_p p_{pb}]\} + \left[1 - \frac{\alpha\left(\frac{m_b + 1}{\chi^{m_b}} B\right)}{q_{ac}}\right]^{n_0} \tag{32}$$

This equation can be solved numerically e.g., by the Runge-Kutta method upon the specification of a single boundary condition.

2.10. Upstream Boundary Condition

[33] Applying an integral version of (23) from the divide to the headwater of the Bedrock River or point of stream inception, it is found that

$$q_b W_b = E_b A_b \tag{33a}$$

$$q_b = E_b \chi_b \tag{33b}$$

where the subscript *b* denotes the origin of a stream [e.g., *Montgomery and Dietrich*, 1988; *Sklar and Dietrich*, 1998] where the incision process in question is found to start at this point toward downstream in the field. A sudden change in slope from the debris flow dominated range ($S \sim$ 0.10–0.40) to the fluvial incision range ($S < 0.10$) [e.g., *Sklar and Dietrich*, 1998] obtained from a longitudinal bed profile, can also guide us regarding this stream inception point in the fluvial system . However, this sudden change in slope may not be generally true everywhere. In the above relations, A_b denotes the area of the drainage basin from the channel inception point (at $x = x_b$) to the divide upstream ($x = 0$) (not necessarily unchannelized, due to other incision processes, e.g., debris flow or suspended-load abrasion). The upstream boundary condition for abrasion and plucking-macroabrasion processes can be determined separately as follows. To obtain the upstream boundary condition for the abrasion part of the model, equations (33a) and (33b) are substituted back into (7) to obtain

$$E_{a.b} = \frac{q_{ac}, b}{\alpha \chi_b}\left[1 - \left(\frac{1}{\beta \alpha \chi_b}\right)^{1/n_0}\right] \tag{34}$$

From (34), for $n_0 = 1$, it is seen that the term $\beta\alpha\chi_b$ must be greater than unity in order to yield a positive value of the incision rate due to abrasion $E_{a.b}$ at the upstream end of the stream. The implication is that if fluvial abrasion is not sufficiently important near the stream head, then the characteristics of the long profile near that point are governed by processes other than fluvial abrasion.

[34] To obtain the upstream boundary condition for the plucking-macro abrasion part of the model, a substitution of (33a) and (33b) back into (19) yields

$$\left(\frac{E_{p,}b}{q_p, bp_{pb,}b}\right)^{1/\mathrm{n}_0} = 1 - \frac{\alpha E_{p,}b\chi_b}{q_{ac}, b} \tag{35}$$

For the case $n_0 \neq 1 = 1$, one obtains

$$E_p, b = \frac{q_{ac,}bq_{p,}bbp_{pb,}b}{q_{ac,}b+\alpha\chi_b q_p, bp_{pb,}b} \tag{36}$$

In the case $n_0 \neq 1$, it is necessary to use an iterative method such as the Newton-Raphson technique to solve for the upstream boundary condition. However, *Chatanantavet and Parker* [2008] found that in general the value $n_0 = 1$ seems reasonable for many cases.

[35] The boundary condition is now formulated for cases in which both abrasion and plucking may be important. In order to do this, it is useful to use the parameter B defined by (30), rather than E itself. From (26) and (30), the sediment transport rate q can be represented in terms of the variable B, and likewise the headwater value q_b can be related to the headwater value B_b as

$$q = \frac{m_b+1}{\chi^{m_b}}\, B \tag{37a}$$

$$q = \frac{m_b+1}{\chi_b^{m_b}}\, B_b \tag{37b}$$

From (33b), (34), (36), (27), and (37b), one finds the upstream boundary condition for (32) in case of $n_0 = 1$ to be

$$B_b = \frac{\chi_b^{m_b}}{m_b+1}\left\{\frac{q_{ac,b}}{\alpha}\left(1 - \left(\frac{1}{\beta\alpha\chi_b}\right)^{1/\mathrm{n}_0}\right) + \frac{q_{ac,b}q_p, bp_{pb,}b\chi_b}{q_{ac,b} + \alpha\chi_b q_p, bp_{pb,}b}\right\} \tag{38}$$

where again m_b, α, β, and *no* are constant and the rest in equation (38) are variable.

2.11. Numerical Model

[36] The sediment transport rate and incision rate along the reach can be calculated using (12a)(12b), (32), (38), (37a), and (7). Then by using the Exner equation (28a), the bed elevation at one time step later can be determined along the reach. The new bed slope at any spatial point can be then calculated. The time evolution of the long profile of the river can then be computed by cycling (12a)(12b), (32), (38), (37a), and (7)for as many time steps as desired. In the case of continuous uplift at a constant rate, the long profile must eventually evolve to an equilibrium (steady) state where the incision rate and uplift rate balance each other everywhere. It

is shown in section 3, however, that transient but nevertheless long-lived autogenic knickpoints may develop during this process.

3. Samples of Model Results

[37] In this section, the model developed in the previous section is run with sample input parameters and the results are shown. Here, we use Excel and Visual Basic for Applications code (VBA) to construct the numerical model. The results are separated into three main sections: (1) the limit of abrasion-dominated incision, (2) the limit of plucking-macroabrasion-dominated incision, and (3) cases for which abrasion and plucking processes both contribute.

[38] The numerical results presented consist of the evolution of the long profiles of bed elevation η, sediment transport q, channel incision rate E, and areal fraction of bedrock exposure p_0. Note that the plots of sediment transport, incision rate, and fraction of bedrock exposure should be considered as the values that prevail during floods when incision is active; during the rest of the time in a year the river is considered to be morphologically inactive. Table 1 below illustrates input parameters used to produce the results in this section. They have been selected to be as representative as possible of at least a subset of field bedrock streams. In some cases, however, independent estimates are not yet available, and as a result values inferred to be reasonable have been selected. An example of such a parameter is the coefficient φ_{ma} characterizing macroabrasion.

Table 1. Input Parameters for Each Section of the Samples of Model Results"

Input Parameters	Run A-1	Run A-2	Run P-1	Run A-P, Default Case
Uplift rate $\boldsymbol{v}$	5mmy^{-1}	5mmy^{-1}	0.1 mm y^{-1}	5mmy^{-1}
Effective rainfall rate $\boldsymbol{i}$	25 mm h^{-1}	25 mm h^{-1}	45 mm h^{-1}	25 mm h^{-1}
Flood intermittency $\boldsymbol{I}$	0.002	0.002	0.001	0.002
Time constant for aging $\boldsymbol{T_{pa}}$	-	-	5000 years	1×10^5 years
Dimensionless parameter for macroabrasion $\boldsymbol{\varphi_{ma}}$	-	-	0.001	-
Effective size of pluckable particles $\boldsymbol{D_p}$	-	-	500 mm	50 mm
Mean grain size that do the wear $\boldsymbol{D_a}$	50 mm	50 mm	-	50 mm
Fraction of coarse grain $\boldsymbol{a}$	0.05	0.05	-	0.05
Bed friction coefficient $\boldsymbol{C_f}$	0.01	0.01	0.01	0.01
Initial bed slope $\boldsymbol{S_{init}}$	0.006	steady state of section 3.1.2 - Figure 4a	0.01	0.006
Initial value of $\boldsymbol{p_{pa}}$, $\boldsymbol{p_{painit}}$	0	0	0.4	0.001
Initial value of $\boldsymbol{p_{pbinit}}$	0	0	0.4	0.001
Thickness of aging layer $\boldsymbol{L_a}$	-	-	10 m	0.4 m
Reach length $\boldsymbol{L}$	10 km	10 km	13 km	10 km
Downstream elevation $\boldsymbol{\eta_{end}}$			0	0
Effective size of particles that do the macroabrasion $\boldsymbol{D_{ma}}$	-	-	150 mm	-
Fraction of load consisting of sizes that do the macroabrasion $\boldsymbol{a_1}$	-	-	0.05	-
Abrasion coefficient $\boldsymbol{\beta}$	0.0002 m^{-1}	0.0001 m^{-1}	1 x 10^{-6} m^{-1}	1 x 10^{-4} m^{-1}
Distance from channel head to	1.5 km	1.5 km	1.5 km	1.5 km

drainage divide upstream x_b				
Coefficient in relation for entrainment of pluckable particles γ_b	-	-	0.0199	0.0199
Exponent in relation for entrainment of pluckable particles n_e	-	-	1.5	1.5
Critical Shields stress in relation for entrainment of pluckable particles τ_{cp^*}	-	-	0.045	0.045
Porosity of bedrock λ_p	0	0	0	0
Exponent in relation governing fraction of the bed not covered by bedrock n_o	1	1	1	1
Coefficient in Hack's Law K_h	6.7	6.7	6.7	6.7
Exponent in Hack's Law n_h	1.7	1.7	1.7	1.7
Coefficient in width relation α_b	0.02	0.02	0.02	0.02
Exponent in width relation n_b	0.4	0.4	0.4	0.4
Coefficient in transport relation for particles doing the wear or macroabrasion γ_t	5.7	5.7	5.7	5.7
Exponent in transport relation for particles doing the wear or macroabrasion n_t	1.5	1.5	1.5	1.5
Critical Shields stress in transport relation for particles doing the wear or macro abrasion τ_c^*	0.04	0.04	0.04	0.04
Height of base level fall at initial time	-	30 m	-	-
Run time	18,000 years	1200 years	600 years	14,400 years

'See section 3.1.1 for Run A-1, section 3.1.3 for Run A-2, section 3.2 for Run P-1, and section 3.3 for Run A-P.

[39] It should be noted that all the runs presented here are performed under the constraint of an imposed, constant value of the abrasion coefficient β. The model of *Sklar and Dietrich* [1998, 2004] allows for a value of β that can change with flow conditions. The framework of the present model, however, allows the incorporation of more general forms for β. *Chatanantavet and Parker* [2006], for example, found that improvement might be needed in regard to the formulation and derivation of the abrasion term (e.g., equation (5)) by *Sklar and Dietrich* [2004], which indicated that the higher the shear stress, the lower incision rate would result. Their model produces results with the opposite trend to experimental erosion rates obtained from a flume with erodible substrate [e.g., *Johnson and Whipple*, 2007; *Chatanantavet and Parker*, 2006].

3.1. Results for Abrasion-Dominated Bedrock Rivers

[40] The results below illustrate the variety of bed elevation profiles resulting from the model applied to abrasion only, using the input parameters in Table 1.

3.1.1. Model Results Yielding Concave-Upward Profiles

[41] This section presents numerical model results for the case of an autogenic concave-upward profile. A concave-upward profile has been claimed by many researchers

[e.g., *Slingerland and Snow*, 1988] to be a necessary (but not sufficient) condition for a steady state where incision balances uplift. The input parameters for the results presented are given in the second column of Table 1 (Run A-1). The incision rates E, E_a and E_p introduced previously all refer to rates during flood events. The corresponding mean annual values are IE, IE_a, and IE_p. From this point on, all incision rates will be presented as mean annual values.

[42] Figures 3a–3d illustrate the results for the time evolution of profiles of bed elevation η, sediment transport rate q, mean annual channel incision rate *IE*, and areal fraction of bedrock exposure p_0, respectively. Figure 3a shows that although the bed profile starts from a channel with constant slope the model develops a concave-upward profile and finally approaches a steady state condition where uplift rate indeed balances incision rate (see Figure 3c). Note that the initial and transient incision rates predicted by the model (Figure 3c) are rather large (~10 mm y^{-1}) due to a relatively high value of the abrasion coefficient (1×10^{-4} m^{-1}). This value reflects weak rocks such as weathered sandstone as suggested by equation (5) in conjunction with *Sklar and Dietrich* [2001]. In time, however, the incision rate comes to be in perfect balance with the uplift rate. Figures 3b and 3d illustrate the downstream increasing trend of sediment transport per unit width and the downstream decreasing trend of the fraction of bedrock exposure, both under transient and equilibrium conditions.

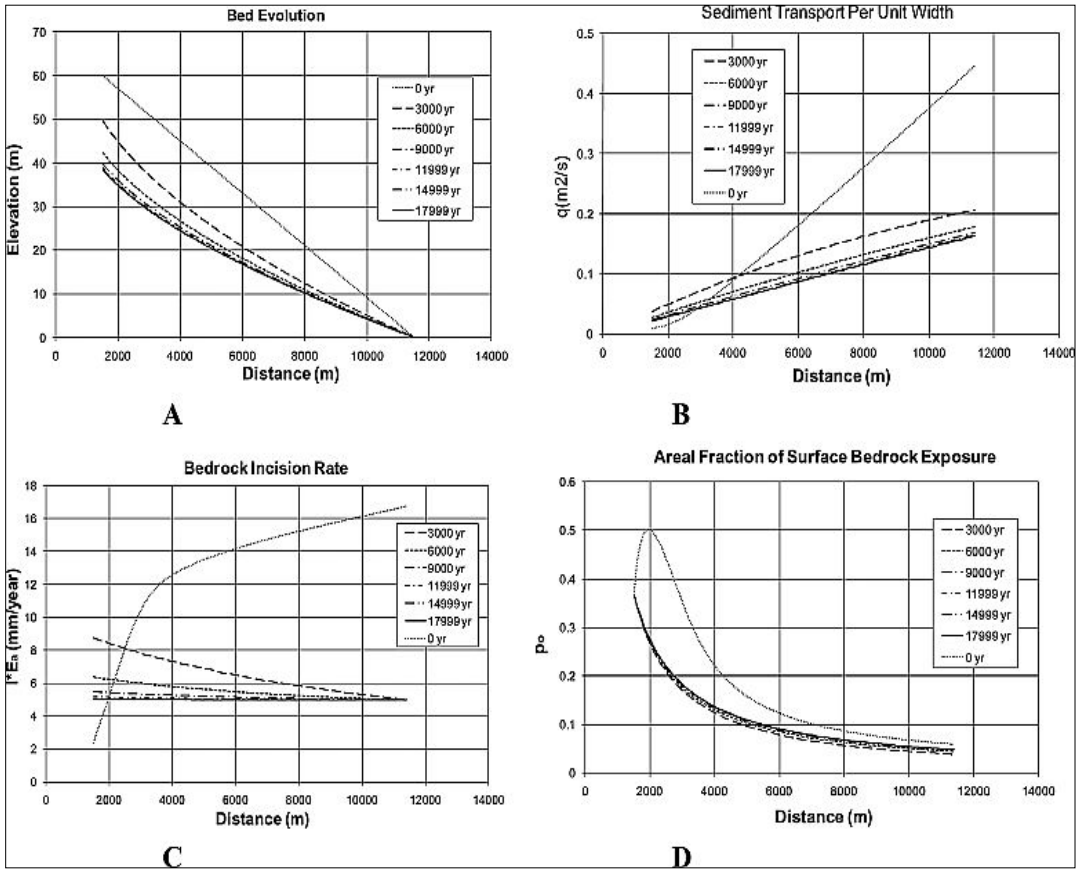

Figure 3.Abrasion-dominated numerical model results showing an autogenic concave-upward profile for (a) bed elevation profile η; (b) sediment transport rate per unit width q; (c) mean annual channel incision rate *IEa*; and (d) areal fraction of surface bedrock exposure p_0. The input parameters are given in the second column of Table 1.

3.1.2. Autogenic Knickpoints

[43] In the next numerical experiment, we investigate a development of autogenic knickpoints found in some model results. The input parameters in this section are the same as those in section 3.1.1 except that the abrasion coefficient, β, is equal to 0.0001 m^{-1}, i.e., half of the value used in section 3.1.1.

[44] Figure 4a generally shows results similar to those of Figure 3a when approaching the steady state condition. Before reaching a concave-upward steady state profile around year 7200, however, the transient bed profiles illustrate an autogenic knickpoint, which propagates upstream and eventually disappears. This autogenic knickpoint is not due to a numerical instability. An analysis of how an autogenic knickpoint develops is presented in section 4. Note that from years 1200 to 3600, the knickpoint elevation is higher than the elevation in the initial year because the channel has been uplifting through time at a rate of 5 mm y^{-1}. Figure 4b illustrates a fraction of bedrock exposure that is higher above the knickpoint and lower below the knickpoint. This is consistent with several field observations [e.g., *Seidl et al.*, 1994; *DeYoung*, 2000; *Crosby and Whipple*, 2005], all of which indicate that below the knickpoint the density of large clasts is much higher than the upstream part above the knickpoint, so protecting the bedrock from incising.

3.1.3. Morphological Changes Caused by a Sudden Base Level Fall

[45] A sudden base level fall in mountain streams can be induced by several natural processes such as sea level fall, stream capture, coseismic or interseismic events (e.g., earthquakes), or catastrophic landslides near the coast. These processes can alter the bed elevation profile of the stream considerably over a relatively short time scale. The response to base level fall is modeled below.

[46] The input parameters in this section are the same as the ones in section 3.1.2 except for one feature. That is, the model is started with a concave-upward profile of the steady state obtained from the run of section 3.1.2 (Figure 4a). At the initial year, the downstream end of the channel experiences a sudden base level fall of 30 m (Figure 5a). The evolution of the bed elevation profile is reminiscent of the channel profiles of some natural bedrock streams which have apparently experienced a sudden base level fall [e.g., *Seidl et al.*, 1994; *DeYoung*, 2000]. Figure 5b shows that incision rates in the earlier years of the model run are higher than in later years, at which an equilibrium state would be approached. The morphological changes seen in Figure 5a occur in a relatively shorter timescale than the ones in sections 3.1.1 and 3.1.2because at the downstream point of base level fall, the channel slope, the shear stress, and thus the incision rate are very high, causing initial rapid incision.

3.2. Results for Plucking-Macroabrasion Dominated Bedrock Rivers

[47] This section presents the numerical model results for the model in the range where plucking-macroabrasion processes dominate. The input parameters are given in the fourth column of Table 1 (Run P-1). The model is run for 600 years in Figure 6, by which time a steady state is almost completely achieved. Note that the incision rates over this short transient period are quite high, with values as high as 20 ~ 90 mm y^{-1}.

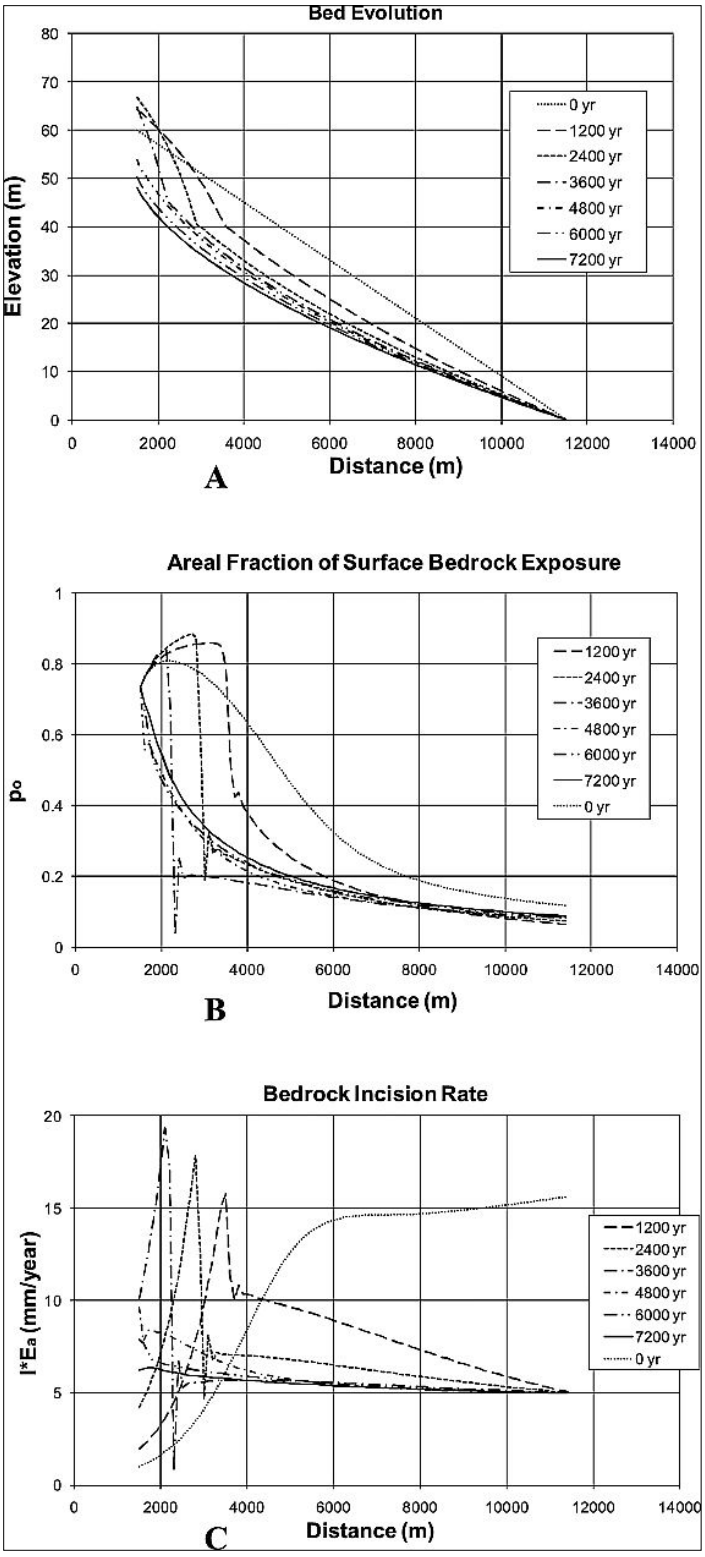

Figure 4. Abrasion-dominated numerical model results showing an autogenic knickpoint propagating upstream for (a) bed elevation profile η; (b) areal fraction of surface bedrock exposure p_0; and (c) mean annual channel incision rate IE_a.

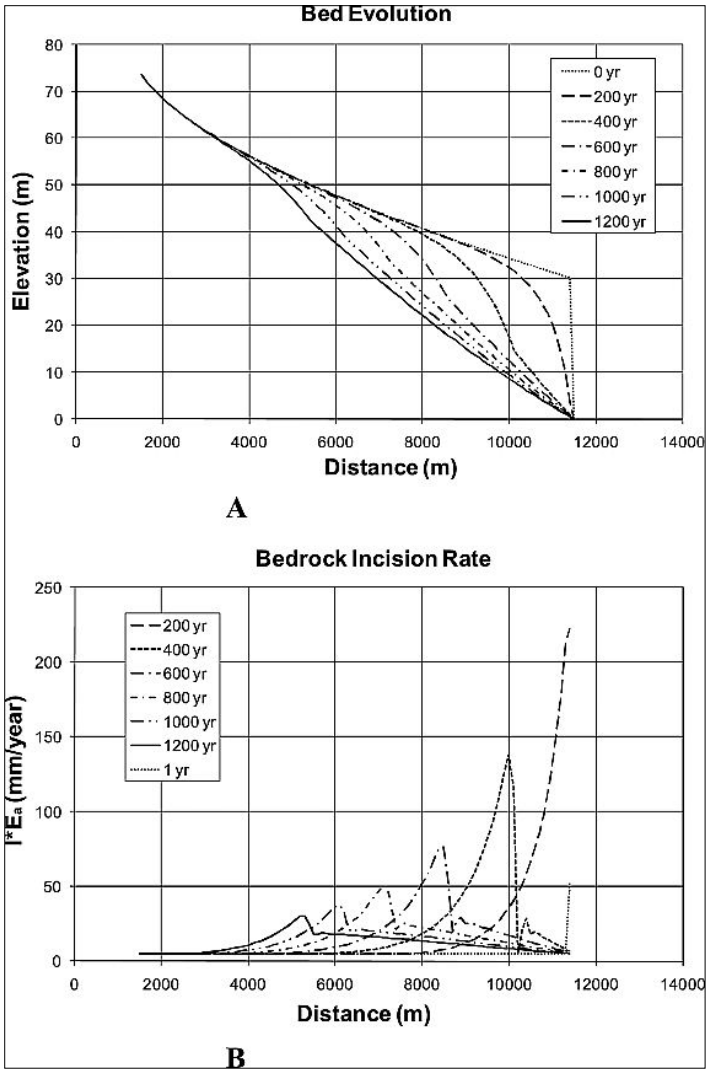

Figure 5. Abrasion-dominated numerical model results showing a knickpoint resulting from a sudden base level fall: (a) bed elevation profile η; and (b) mean annual channel incision rate IE_a.

[48] The model results show an autogenic knickpoint (the point where channel slope suddenly changes in Figure 6c) propagating upstream with a concave-upward channel segment in the downstream part (Figures 6a and 6c), a feature of plucking-dominated bedrock channels that is studied in Orchha River of Abujhmarh. and the Unnamed Drainage #1, Achal .Meta. We observed a high magnitude of incision rate due to plucking (50–200 mm y^{-1}) in Orchha gorge, and also documented high incision rates of 10–100 mm y^{-1} in the un named River, in which the plucking of joint blocks was observed. Note that the input value for the dimensionless macroabrasion parameter, φ_{ma}, i.e., 0.001, represents a reasonable guess based on several trial runs but is yet to be determined in the future.

[49] It is observed in the field that in many plucking-dominated bedrock streams, a horseshoe-shaped lip of knickpoints, a stable form that persists as knickpoints migrates upstream, is prevalent because this planform distributes shear stress uniformly..

3.3. Results for the Case of Combined Abrasion and Plucking

[50] In this section, parameters are selected so that abrasion and plucking processes both affect the evolution of the incision process. Macroabrasion is omitted here so as to highlight the competition between abrasion and plucking processes. Generally, the dominant incision process depends primarily on substrate lithology and can be discerned in the field through the examination of joint spacing [e.g., *Whipple et al.*, 2000a]. Channels formed in resistant, jointed bedrock commonly occur in crystalline lithologies in a wide range of climatic and tectonic settings [*Dubinski and Wohl*, 2005]. An example of the coexistence of incision by both abrasion and plucking processes is that in some bedrock rivers, there are sites where pothole abrasion removes sufficient mass from a large jointed block to enhance the block's susceptibility to lift force and quarrying (E. Wohl, personal communication, 2009).

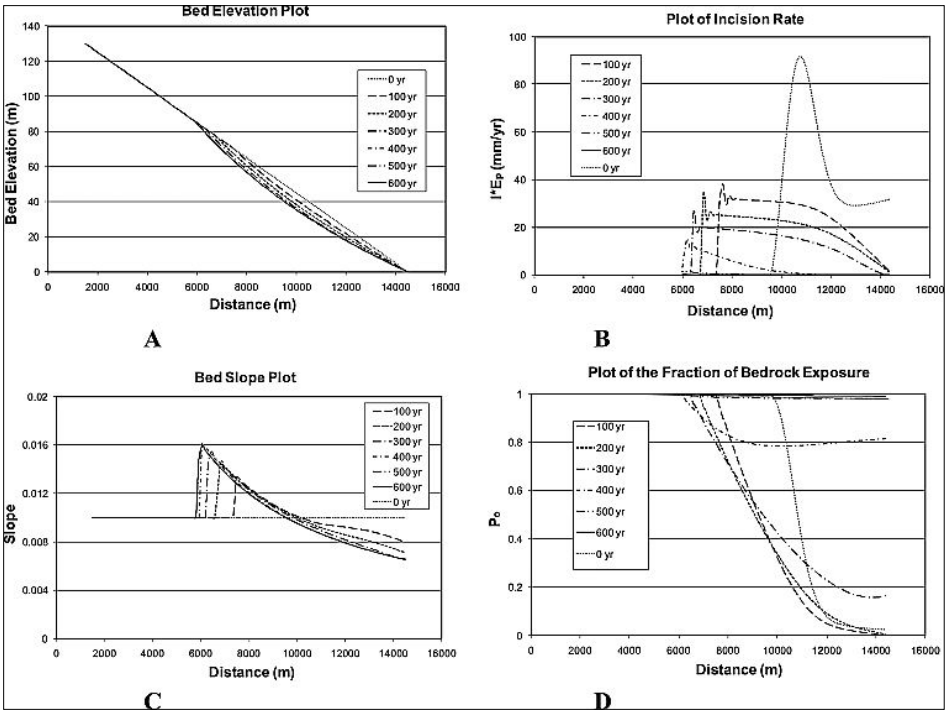

Figure 6. Plucking-macroabrasion-dominated numerical model results showing an autogenic knickpoint propagating upstream and concave-upward downstream segment: (a) bed elevation η; (b) mean annual channel incision rate *IEp*; (c) channel slope *S*; and (d) areal fraction of surface bedrock exposure p_0.

[51] The input parameters in this section are described in the last column of Table 1 (Run A-P). Note that the input parameters in this case are almost identical to the ones in section 3.1.2 (case with autogenic knickpoints) except that the input parameters for plucking processes are added. The values given there in fact describe a default case. Variations from the default case are presented in this section as well.

[52] Although both abrasion and plucking proceed simultaneously and interact nonlinearly in the calculation based on the default parameters, it is still possible to compute the part of the total incision rate *E* due to abrasion alone, i.e., *Ea*, and that part due to plucking, *Ep*, in accordance with (7), (19), and (27). Figures 7a and 7b show the time evolution of profiles of incision rate due to abrasion and plucking, respectively. It is seen there that at steady state, about forty percent of the incision is driven by plucking, with the remainder driven by abrasion. The

plots of incision rates both during transient state and at steady state thus can guide us whether or not both abrasion and plucking processes operate on the channel in question. The time evolution of the long profile is shown in Figure 7c. The results in this case are different from the case of abrasion-dominated channels (i.e., section 3.1.2 and Figure 4) in that (1) the rate of bed lowering is faster (i.e., comparing the bed profiles in Figure 4a and Figure 7c at year 7200) and (2) there is no autogenic knickpoint (see explanation in section 4).

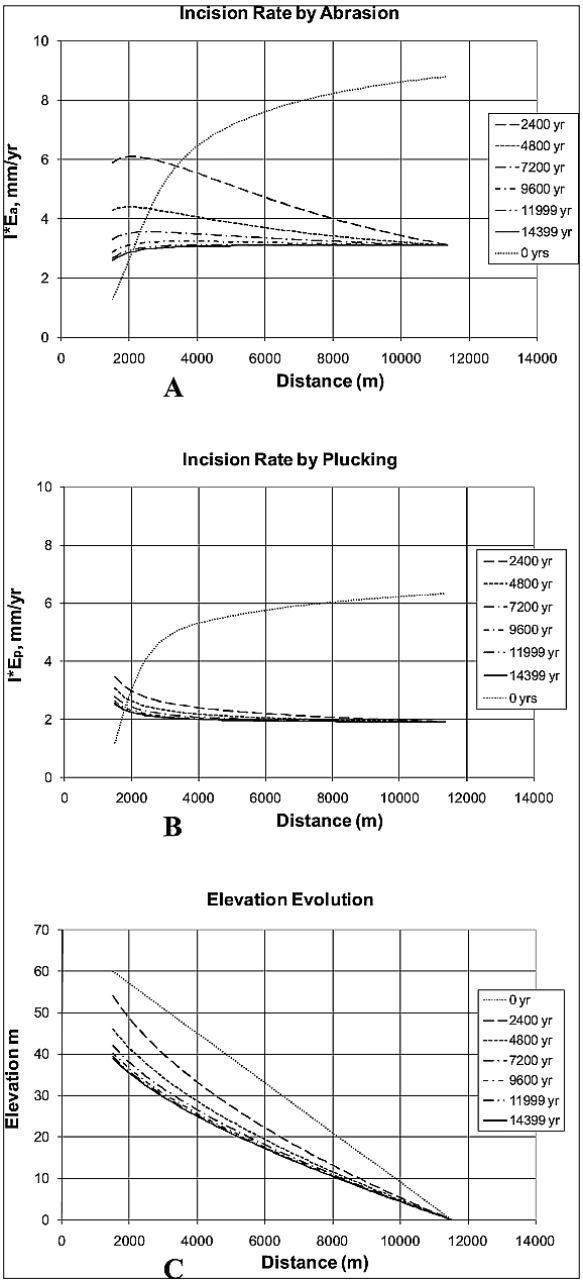

Figure 7. Results for the default case (last column of Table 1) with both plucking and abrasion: (a) mean annual incision rate *IEa* due to abrasion; (b) mean annual incision rate *IEp* due to plucking; and (c) evolution of bed elevation η.

[53] For the default case, the abrasion coefficient β takes the rather high value of 1×10^{-4} m^{-1}. Figures 8a–8c illustrate the case where the input parameters are the same as the default

case except that the abrasion coefficient is reduced to be 1×10^{-5} m^{-1} (e.g., harder rock). In this case, the incision rate by abrasion is about one order of magnitude less than the default case (Figure 8a) while the incision rate by plucking increased to take up the difference in balancing against the uplift rate at steady state (Figure 8b).

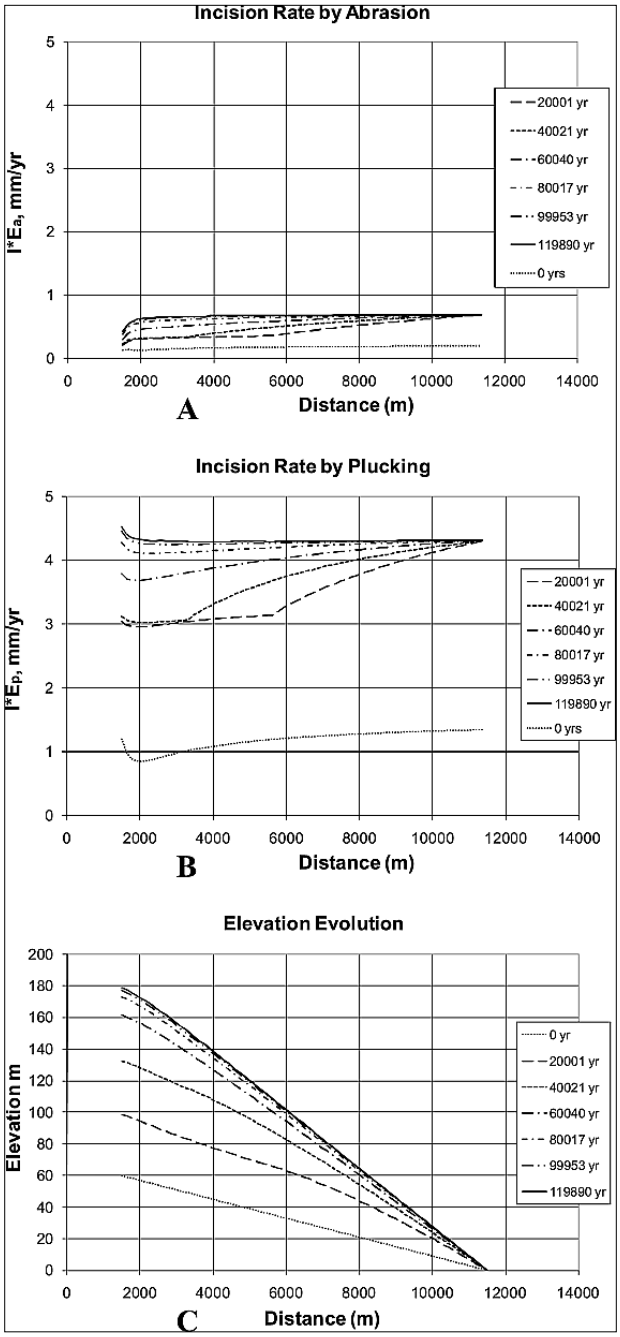

Figure 8. Incision rates due to abrasion and plucking for the case of abrasion coefficient reduced to 1×10^{-5} m^{-1} (with other parameters remaining the same as the default case): (a) mean annual incision rate *IEa* due to abrasion; (b) mean annual incision rate *IEp* due to plucking; and (c) evolution of bed elevation η.

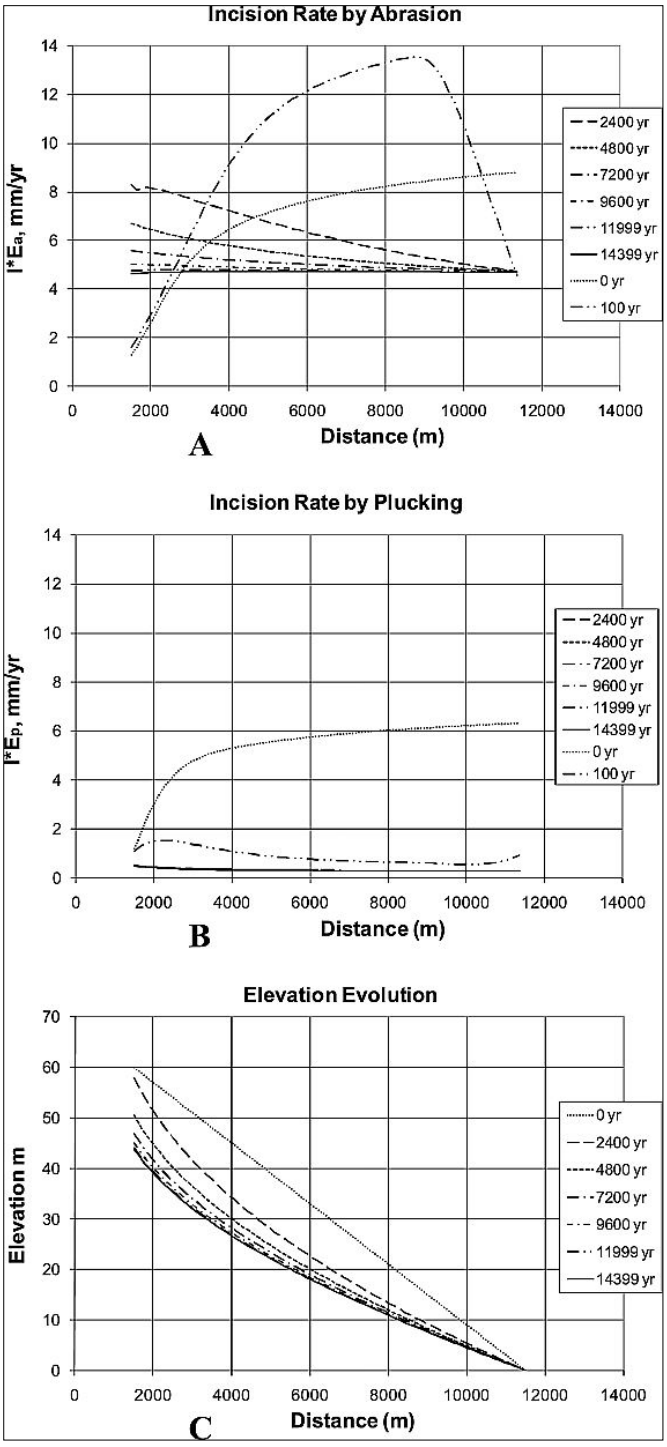

Figure 9. Incision rates due to abrasion and plucking for the case of aging time (Tpa) = 1×10^6 years (with other parameters remaining the same as the default case): (a) mean annual incision rate IE_a due to abrasion; (b) mean annual incision rate *IEp* due to plucking; and (c) evolution of bed elevation η.

Owing to the high uplift rate of 5 mm y^{-1} and the relatively lower incision rate by plucking during the transient state (comparing to the abrasion counterpart), the bed elevation profile is uplifted (Figure 8c) as it approaches a steeper steady state, resulting in a convex-upward profile during the

transient state. This steady state requires ~100,000 years to obtain, as opposed to ~10,000 years for the default state. The run illustrates how the incision process in which abrasion and plucking are of similar importance can be changed to one for which plucking dominates simply by reducing the abrasion coefficient by an order of magnitude.

[54] Figures 9a–9c illustrate the case where the input parameters are the same as the default case except that the aging time T_{pa} is increased to 10^6 years rather than the value of 10^5 years of the default case. In this case, the part of the incision rate due to plucking quickly drops to about one order of magnitude less than the default case (Figure 9b), while the part of the incision rate by abrasion increases to take up the difference in balancing uplift (Figure 9a). It is also seen that incision by abrasion thus drives most of the incision during the transient state.

4. Discussion

[55] In this study, we have shown that our physically based bedrock incision model is able to simulate various common steady state and transient features of the bed elevation profiles of bedrock rivers such as (1) transient and steady state concave-upward profiles, (2) concave-upward profiles with a transient propagating convex knickpoint for the case of domination by abrasion, (3) concave-upward profiles with a propagating knickpoint in case of domination by plucking and macroabrasion, and (4) profiles with a transient propagating allogenic knickpoint resulting from an imposed sudden base level fall.

[56] The bed profile consisting of a propagating knickpoint with a concave-upward channel segment downstream produced by the plucking-macroabrasion model is consistent not only with field data [e.g., *Tinkler and Parish*, 1998; *Miller*, 1991] but also with experimental work of knickpoint propagation in a flume filled with pluckable blocks by *Dubinski and Wohl* [2005]. The model results also demonstrate that the bed morphology resulting from incision by plucking-macroabrasion processes can operate on a shorter time scale (i.e., 10^1–10^2 years) than the abrasion counterpart (i.e., 10^3–10^6 years). This is because the block-by-block removal in the plucking process can produce higher incision depth per year than abrasion from clasts into silt or sand. In order for plucking to be effective, however, (1) pluckable blocks need to be available, and (2) the flow needs to be competent to move these blocks.

[57] The competition between incision by bed load abrasion and plucking processes has been demonstrated in section 3.3. The results suggest that, among other parameters, a higher value of the abrasion coefficient (β), which means weaker rock (lower tensile rock strength) leads to more pronounced incision by abrasion, while a shorter aging time (T_{pa}) of bedrock leads to more pronounced incision by plucking and macroabrasion. These two parameters seem to be the key parameter governing the dominance of the incision processes whether it be abrasion-dominant or plucking-dominant in a bedrock channel. From the numerical results in section 3.3, nonlinear interaction between the abrasion and plucking processes (and thus macroabrasion) should be expected. The nonlinear interaction can be described as follows. When channel incision (by any processes) occurs, the hillslope materials are pulled down and delivered into the channel ((23) and (26)). These materials then become bed load and facilitate the macroabrasion process (17), increasing the incision rate by plucking. Also, the plucked particles, which become bed load, can buffer the bed as in the cover term (6), preventing further incision by both bed load abrasion and plucking.

[58] Regarding the results in Figure 9 (section 3.3), unlike the case when the plucking process dominates (Figure 8), where the bed profile is constantly uplifted due to the low incision

rate by plucking during the transient state and the high uplift rate (Figure 8c), the bed elevation profile in Figure 9c still develops a concave-upward form throughout the evolution since the incision rates by abrasion during the transient state are consistently high. When the bedrock incision by abrasion is suppressed (e.g., in case of harder rocks) and plucking process dominates such as in Figure 8c, although the incision by plucking is balancing the uplift rate at steady state, during the transient state the incision by plucking process may not be efficient enough (or efficient only in the first hundreds of years e.g., Figure 6c) to drive high channel incision rate to keep pace with the uplift rate and to develop a concave-upward profile. This, however, may be exempted in the case of fracturing due to an external forcing such as wetting and drying [e.g., *Tinkler and Parish*, 1998] where the aging time could be in the shorter timescale of decades or less.

[59] The model applied in the regime of abrasion dominance demonstrates that convex-upward knickpoints found in natural bedrock rivers may be autogenic in addition to being allogenically driven by a base level fall or lithologic changes. The analysis of the formation of an autogenic knickpoint can be described as follows. From the Exner equation (28a), taking the second derivative in x and assuming a constant and uniform rock uplift rate and a zero value of porosity results in

$$\frac{\partial}{\partial t}\left(\frac{\partial^2 \eta}{\partial x^2}\right) = -I\frac{\partial^2 E}{\partial x^2} \tag{39a}$$

$$\frac{\partial}{\partial t}\left(\frac{\partial S}{\partial x}\right) = -I\frac{\partial^2 E}{\partial x^2} \tag{39b}$$

Now consider the plot of the incision rate in Figure 4c at year zero. Note that the shape of the curve of the incision rate Ea changes from concave-upward upstream to convex-upward downstream at a point near the distance 4000 m (the inflection point). Thus the term $\partial^2 E/\partial x^2$ changes from positive to negative near this point. Considering (39a), a stream with such a shape of the incision curve must gradually form an autogenic knickpoint such that the term $\partial^2 \eta/\partial x^2$ has the opposite sign of $\partial^2 E/\partial x^2$. This results in an elevation curve that changes from upward convex in the upstream reach to upward concave in the downstream reach. The point of the shock condition (knickpoint) then automatically migrates upstream (Figure 4a). Note that the size of an autogenic knickpoint (i.e., its height) can vary depending on the input parameters.

[60] In Figure 3c, on the other hand, there is no point of inflection in the initial profile of the incision rate. The incision plot shows only a convex-upward profile. Therefore the term $\partial^2 E/\partial x^2$ has only negative values, resulting in only positive values of the term $\partial^2 \eta/\partial x^2$ and thus no autogenic knickpoint formation. The lack of point of inflection in the initial profile of the incision rate in Figure 3c is due to the fact that different values of input parameters (e.g., β or α) can potentially and nonlinearly alter the initial profile of incision rate and that incision rates at any point in the channel depend on the ones upstream, as shown in equation (29).

[61] Considering equation (39b), one might notice a resemblance of this equation with a wave equation, as slope on the left-hand side could be viewed as a component in determining incision rate. The generation of an autogenically propagating knickpoint, which has a wave-like feature, may thus be implicit in this equation. Major parameters such as β and α, which directly link slope to incision rate, therefore have an impact on the occurrence of the autogenic knickpoint.

[62] Regarding the results that show no autogenic knickpoint for the case of combined abrasion and plucking processes (section 3.3 and Figure 7) although the input parameters for

abrasion are identical to section 3.1.2 (Figure 4) in which an autogenic knickpoint is generated, it can be explained as follows. First of all, one may wonder why while there is an inflection point in the initial profile of the incision rate in Figure 4c, there is none in Figure 7a for the initial profile of the incision by abrasion. According to equation (29), incision rate due to abrasion at any point in the channel is a function of incision due to all processes (including plucking and macroabrasion) in the upstream area of that point. Since in Figure 7 plucking process is also considered, it affects the incision rate by abrasion at initial time. To test this claim, we ran the model in section 3.3 again but with $Tpa = 10^9$ years and initial values of ppa and $ppb = 10^{-5}$ in order to suppress the plucking process. As expected, the autogenic knickpoint was generated and all the results were similar to ones in section 3.1.2.

5. Conclusion

[63] The physically based incision model presented here is developed to seek a complete framework for bedrock incision by bed load abrasion, plucking, and macroabrasion processes. All parameters used in the model have physically meaningful dimensions and are quantifiable in the field or laboratory, which are advantageous compared to previous bedrock incision models.

[64] To build the model, we start by developing a theory describing abrasion, plucking, and macroabrasion mechanisms. We then incorporate hydrology, the evaluation of boundary shear stress, a quantification of capacity transport, an entrainment relation for pluckable particles, a routing model linking in-stream sediment transport and hillslope delivery, a formulation for alluvial channel coverage, a channel width relation, Hack's law, and the Exner equation into the model so that we can simulate the evolution of bedrock channels. The model is implemented for a variety of cases, in order to study both steady state and the evolution toward steady state in (1) abrasion-dominated channels, (2) plucking-macroabrasion-dominated channels, and (3) channels in which both abrasion and plucking are important. The model can simulate various general features of the bed elevation profiles of bedrock rivers and provides the numerical results pertaining to the spatial and temporal variation of bed elevation η, channel slope S, mean annual bedrock incision rate IE, sediment transport rate per unit width q, and areal fraction of bedrock exposure po.

[65] Future research could include the verification in the field or laboratory of the autogenic knickpoint generated by the abrasion-dominated model. A more detailed investigation of the dimensionless macroabrasion coefficient in order to better understand the physics behind this process should also be done in future research. It is hoped that our work represents a step closer to modeling landscape evolution with more detailed physics underpinning the modeling of bedrock incision processes.

Notation

A drainage area; equation (11).
A_b drainage area at the upstream boundary of the channel (channel head); equation (33).
A_p surface area of a pluckable particle; equation (15).
B an auxiliary variable in solving the differential equation of bedrock incision (29) numerically; equation (30).
B_b the value of auxiliary variable at the upstream boundary (channel head); equation (38).
C_f a friction coefficient; equation (9).
D_a a characteristic size of the saltating grain that do the wear or abrasion; equation (8).
D_{ma} mean size of particles that do the macroabrasion by hitting the bed and inducing cracks; equation (15).

D_p a characteristic size of pluckable stone; equation (14).
E total vertical bedrock incision rate by all processes; equation (13).
E_a rate of bedrock incision due to wear or abrasion; equation (3).
$E_{a,b}$ rate of bedrock incision due to wear or abrasion at the upstream boundary of the channel (channel head); equation (34).
E_b total vertical bedrock incision rate at the upstream boundary of the channel (channel head); equation (33).
E_k total vertical bedrock incision rate resulting from a flow range k; equation (28b).
E_p rate of bedrock incision due to plucking (and macroabrasion); equation (19).
$E_{p,b}$ rate of bedrock incision due to plucking (and macroabrasion) at the upstream boundary of the channel (channel head); equation (35).
g acceleration of gravity; equation (8).
H average flow depth; equation (9).
i precipitation rate; equation (11).
I flood intermittency; equation (13).
I_k flood intermittency in the kth flow range; equation (28b).
k flood flow range; equation (28b).
K_v dimensionless rock resistance constant; equation (5).
K_h coefficient in Hack's relation; equation (25).
L_a thickness of aging layer; equation (13).
L_s characteristic saltation length of wear particles; equation (2).
m_b an exponent defined as $m_b = n_b/(1 - n_b)$; equation (24).
n_b an exponent in width-area relation; equation (24).
n_E a dimensionless exponent in the entrainment relation of pluckable particles; equation (18).
n_h an exponent in Hack's relation; equation (25).
n_o an exponent in the equation of cover factor of alluvial deposit; equation (6).
n_T a dimensionless exponent in Meyer-Peter and Müller transport capacity formula; equation (8).
p_o areal fraction of surface bedrock that is not covered with wear particles; equation (6).
p_{pa} volume fraction of material in the aging layer that has broken up into pluckable chunks; equation (13).
p_{painit} volume fraction of material in the aging layer that has broken up into pluckable chunks at the initial time of a numerical model run.
p_{pb} volume fraction of material in the battering layer that consists of pluckable particles; equation (14).
p_{pbinit} volume fraction of material in the battering layer that consists of pluckable particles at the initial time of a numerical model run.
$p_{pb,b}$ volume fraction of material in the battering layer that consists of pluckable particles at the channel head; equation (35).
q total volume sediment transport rate per unit width; equation (1).
q_a volume transport rate per unit width of sediment coarse enough to abrade the bedrock; equation (1).
q_{ac} capacity transport rate of wear particles; equation (6).
$q_{ac,b}$ capacity transport rate of wear particles at the upstream boundary (channel head); equation (34).
q_b undary of the channel (channel head); equation (33).
q_h volume of sediment per stream length per unit time entering the channel from the hillslopes; equation (21).
$q_p$volume rate of entrainment of pluckable chunks into bed load transport per unit bed area per unit time; equation (18).

$q_{p,b}$volume rate of entrainment of pluckable chunks into bed load transport per unit bed area per unit time at the channel head; equation (35).
$q_w$flow discharge per unit width; equation (9).
r fraction of the particle volume ground off the bed in each collision; equation (3).
R nondimensional buoyant density = $(\rho_s/\rho) - 1$; equation (8).
S channel slope; equation (10).
S_{init} initial slope specified in the numerical model.
t time; equation (13).
T_{pa} aging time; equation (13).
T_{pb} time associated with enhanced breakup due to macroabrasion in the battering layer; equation (14).
U mean flow velocity.
V_a volume of a wear particle; equation (3).
V_{ma}volume of a wear particle big enough to hit the bed strongly resulting in cracking and eventually macroabrasion; equation (15).
W channel width; equation (11).
W_b channel width at the upstream boundary of the channel (channel head); equation (33).
w_{si} vertical sediment impact velocity; equation (5).
x down channel distance along the stream; equation (21).
Y Young's modulus of elasticity of rock; equation (5).
a fraction of load that consists of particles coarse enough to do the wear; equation (1).
α_1 fraction of load that consists of particles coarse enough to do the macroabrasion.
α_b a coefficient in width-area relation; equation (24).
$\breve{\alpha}_b$ a coefficient defined as $\breve{\alpha}_b = \alpha_b^{1(1-n_b)}$ equation (24).
β abrasion coefficient [1/L]; equation (4).
ζ the volume rate at which saltating wear particles bounce off the bed per unit bed area; equation (2).
η elevation of the river bed; equation (28).
η_{end} downstream elevation of the river.
γ_E a dimensionless constant in the entrainment relation of pluckable particles; equation (18).
γ_T a dimensionless constant in Meyer-Peter and Müller transport capacity formula; equation (8).
φ_{ma} dimensionless parameter characterizing macroabrasion; equation (17).
χ a surrogate for distance x defined as $\chi = A/W$; equation (12).
χ_b a surrogate for distance x at the upstream boundary (channel head) as $\chi_b = A_b/W_b$; equation (33).
λ_p porosity of bedrock; equation (28).
υ uplift rate; equation (28).
ρ water density; equation (8).
ρ_s rock density; equation (5).
σ_T rock tensile strength; equation (5).
τ_b bed shear stress; equation (8).
τ_c^* a dimensionless critical Shields number; equation (8).
τ_{cp}^* a critical Shields number for entrainment of pluckable grains; equations (18a)–(18b).

References

Bitter, J. G. A. (1963a), A study of erosion phenomena, part I, *Wear, 6,* 5-21,doi:10.1016/0043-1648(63)90003-6.

Bitter, J. G. A. (1963b), A study of erosion phenomena, part II, Wear, 6, 169-190, doi:10.1016/0043-

Chatanantavet, P., and G. Parker (2006), Experimental studies on the rate of incision by saltating abrasion:

Verification, analysis, and revision of a physically based model, *Eos Trans. AGU,* 87(52), Fall Meet. Suppl.,Abstract H21E-1423.

Chatanantavet, P., and G. Parker (2008), Experimental study on bedrock channel alluviation under varied Sediment supply and hydraulic conditions, *Water Resour. Res., 44,* W12446, doi: 10.1029/ 2007W R006581.

Crosby, B., and K. X. Whipple (2005), Bedrock river incision following aggradation: Observations from the Waipaoa River regarding tributary response to mainstem incision and the role of paleotopography, *Eos Trans. AGU,* 86(52), Fall Meet. Suppl., Abstract H31A-1263.

DeYoung, N. V. (2000), Modeling the geomorphic evolution of western Kaua'i, Hawai'i: A study of surface processes in a basaltic terrain, Master's thesis, Dalhousie Univ., Halifax, Nova Scotia, Canada.

Dubinski, I. M., and E. E. Wohl (2005), Physical model ofriver erosion into jointed bedrock through ‘ quarrying, *Eos Trans. AGU,* 86(52), Fall Meet. Suppl., Abstract H53D-0516.

Fernandez Luque, R., and R. van Beek (1976), Erosion and transport of bed-load sediment, *J. Hydraul. Res., 14,* 127-144.

Finnegan, N. J., L. S. Sklar, and T. K. Fuller (2007), Interplay of sediment supply, river incision, and channel morphology revealed by the transient evolution of an experimental bedrock channel, *J. Geophys. Res., 112*, F03S11, doi:10.1029/2006JF000569.

Foley, M. G. (1980), Bedrock incision by streams, *Geol. Soc. Am. Bull., 91,* 2189-2213.

Gasparini,N.M.,R.L.Bras,andK.X.Whipple(2006),Numerical modeling of non-steady-state river profile evolution using a sediment-flux-dependent incision model, in *Tectonics, Climate and Landscape Evolution,* edited by S. Willett et al., *Geol. Soc. Am. Spec. Pap., 398,* 127-141.

Gasparini, N. M., K. X. Whipple, and R. L. Bras (2007), Predictions of steady state and transient landscape morphology using sediment-flux-dependent river incision models, *J. Geophys. Res., 112,* F03S09, doi:10.1029/2006JF000567.

Hack, J. T. (1957), Studies of longitudinal stream profiles in Virginia and Maryland, *U.S. Geol. Soc. Prof Pap., 294-B,* 45-97.

Johnson, J. P. (2007), Feedbacks between erosional morphology, sediment transport and abrasion in the transient adjustment of fluvial bedrock channels, Ph.D. dissertation, Mass. Inst. of Technol., Cambridge, Mass.

Johnson, J. P., and K. X. Whipple (2007), Feedbacks between erosion andsediment transport in experimental bedrock channels, *Earth Surf. Processes Landforms, 32,* 1048-1062, doi:10.1002/esp.1471.

Lamb, M. P., W. E. Dietrich, and L. S. Sklar (2008), A model for fluvial bedrock incision by impacting suspended and bedload sediment, *J. Geo-phys. Res., 113,* F03025, doi:10.1029/2007JF000915.

Maritan, A., A. Rinaldo, R. Rigon, A. Giacometti, and I. Rodriguez-Iturbe (1996), Scaling law for river network, *Phys. Rev. E, 53,* 1510-1515,doi:10.1103/PhysRevE.53.1510.

Meyer-Peter, E., and R. Miiller (1948), Formulas for bedload transport, Int. Assoc. of Hydraul. Eng. and Res., Stockholm.

Miller, J. R. (1991), The influence of bedrock geology on knickpoint development and channel-bed degradation along downcutting streams in south-central Indiana, *J. Geol., 99,* 591-605, doi:10.1086/629519.

Montgomery, D. R., and W. E. Dietrich (1988), Where do channels begin?, *Nature,* 336(6196), 232-234, doi:10.1038/336232a0.

Montgomery, D. R., and K. B. Gran (2001), Downstream variations in the width of bedrock channels, *Water Resour. Res., 37*(6), 1841 -1846, doi: 10.1029/2000WR900393.

Parker, G. (1991), Selective sorting and abrasion of river gravel I: Theory, *J. Hydraul. Eng.,* 117(2), 131-149, doi:10.1061/(ASCE)0733- 9429(1991)117:2(131).

Rigon, R., I. Rodriguez-Iturbe, A. Maritan, A. Giacometti, D. G. Tarboton, and A. Rinaldo (1996), On Hack's law, *Water Resour. Res., 32*(11),3367-3374, doi:10.1029/96WR02397.

Rigon, R., I. Rodriguez-Iturbe, and A. Rinaldo (1998), Feasible optimality implies Hack's law, *Water Resour. Res.,* 34(11), 3181-3190,doi:10.1029/98WR02287.

Seidl, M. A., W. E. Dietrich, and J. W. Kirchner (1994), Longitudinal profile development into bedrock: An analysis of Hawaiian channels, *J. Geol., 102,* 457-474, doi:10.1086/629686.

Sklar, L. S., and W. E. Dietrich (1998), River longitudinal profiles and bedrock incision models: Stream

power and the influence of sediment supply, in *River Over Rock: Fluvial Processes in Bedrock Channels, Geophys. Monogr. Ser.,* vol. 107, edited by K. Tinkler and E. E. Wohl, pp. 237-260, AGU, Washington, D. C.

Sklar, L. S., and W. E. Dietrich (2001), Sediment and rock strength controls on river incision into bedrock, *Geology, 29,* 1087-1090, doi:10.1130/ 0091-7613(2001)029<1087:SARSCO>2.0.CO;2.

Sklar, L. S., and W. E. Dietrich (2004), A mechanistic model for river incision into bedrock by saltating bed load, *Water Resour. Res., 40,* W06301, doi:10.1029/2003WR002496.

Slingerland, R. L., and R. S. Snow (1988), Stability analysis of a rejuvenated fluvial system, *Z. Geomor phol.* , *67,* 93 -102.

Slingerland, R., S. D. Willett, and H. L. Hennessey (1997), A new fluvial bedrock incision model based on the work-energy principle, *Eos Trans.AGU, 78,* Fall Meet. Suppl., F46.

Stark, C. P. (1991), An invasion percolation model of drainage network evolution, *Nature, 352,* 423-425, doi:10.1038/352423a0.

Stark, C. P., and G. J. Stark (2001), A channelization model of landscape evolution, *Am. J. Sci., 301,* 486-512, doi:10.2475/ajs.301.4-5.486.

Stark, C. P., E. Foufoula-Georgiou, and V. Ganti (2009), A nonlocal theory of sediment buffering and bedrock channel evolution, *J. Geophys. Res.,114,* F01029, doi:10.1029/2008JF000981.

Tinkler, K. J., and J. Parish (1998), Recent adjustments to the long profile of Cooksville Creek, an urbanized bedrock channel in Mississauga, Ontario, in *River Over Rock: Fluvial Processes in Bedrock Channels, Geophys. Monogr. Ser.,* vol. 107, edited by K. Tinkler and E. E. Wohl, pp. 167-187, AGU, Washington, D. C.

Tomkin, J. H., M. T. Brandon, F. J. Pazzaglia, J. R. Barbour, and S. D. Willett (2003), Quantitative testing of bedrock incision models for the Clearwater River, NW Washington State, *J. Geophys. Res., 108*(B6), 2308, doi:10.1029/2001JB000862.

Tsujimoto, T. (1999), Sediment transport processes and channel incision: Mixed size sediment transport, degradation and armoring, in *Incised River Channels,* edited by S. E. Darby and A. Simon, chap. 3, pp. 3766, John Wiley, Hoboken, N. J.

Tucker, G. E., and R. L. Slingerland (1994), Erosional dynamics, flexural isostasy, and long-lived escarpments, *J. Geophys. Res., 99*,12,22912,243, doi:10.1029/94JB00320.

Turowski, J. M., D. Lague, and N. Hovius (2007), Cover effect in bedrock abrasion: A new derivation and its implications for the modeling of bedrock channel morphology, *J. Geophys. Res., 112,* F04006, doi:10.1029/2006JF000697.

Turowski, J. M., N. Hovius, H. Meng-Long, D. Lague, and C. Men-Chiang (2008), Distribution of erosion across bedrock channels, *Earth Surf. Processes Landforms, 33,* 353-362, doi:10.1002/esp.1559.

Whipple, K. X. (2004), Bedrock rivers and the geomorphology of active orogens,*Annu. Rev. Earth Planet. Sci.,32*,151 -185,doi:10.1146/annurev.earth.32.101802.120356.

Whipple, K. X., and G. E. Tucker (1999), Dynamics of the stream-power river incision model: Implications for height limits of mountain ranges, landscape response timescales, and research needs, *J. Geophys. Res., 104,* 17,661 -17,674, doi:10.1029/1999JB900120.

Whipple, K. X., and G. E. Tucker (2002), Implications of sediment-flux dependent river incision models for landscape evolution, *J. Geophys. Res.,* 107(B2), 2039, doi:10.1029l2000JB000044.

Whipple, K. X., G. S. Hancock, and R. S. Anderson (2000a), River incision into bedrock: Mechanics and relative efficacy of plucking, abrasion, and cavitation, *Geol. Soc. Am. Bull.,* 112(3), 490-503, doi:10.1130l0016-7606(2000) 112<0490:RIIBMA>2.3.CO;2.

Whipple, K. X., N. P. Snyder, and K. Dollenmayer (2000b), Rates and processes of bedrock incision by the Upper Ukak River since the 1912 Novarupta ash flow in the Valley of Ten Thousand Smokes, Alaska, *Geology,* 28(9), 835-838, doi:10.1130l0091-7613(2000)28<835:RAPOBI>2.0.CO;2.

Willett, S. D. (1999), Orogeny and orography: The effects of erosion on the structure of mountain belts, *J. Geophys. Res., 104,* 28,957-28,981, doi:10.1029l1999JB900248.

Willgoose, G., R. L. Bras, and I. Rodriguez-Iturbe (1991), A coupled channel network growth and hillslope evolution model: 1. Theory, *Water Resour. Res.,* 27(7), 1671-1684, doi:10.1029l91WR00935.

Wobus, C. W., J. W. Kean, G. E. Tucker, and R. S. Anderson (2008), Modeling the evolution of channel shape: Balancing computational efficiency with hydraulic fidelity, *J. Geophys. Res., 113,* F02004, doi:10.1029l2007JF000914.

Wohl, E. E., and G. C. L. David (2008), Consistency of scaling relations among bedrock and alluvial channels, *J. Geophys. Res.* , *113,* F04013, doi:10.1029l2008JF000989.

Woodford, A. O. (1951), Stream gradients and Monterey Sea Valley, *Geol.Soc.Am.Bull, 62,* 799-852,

P. Chatanantavet, School of Earth and Space Exploration, Arizona State University, Tempe, AZ 85287, USA. (pchatana@mainex1.asu.edu)
G. Parker, Department of Civil and Environmental Engineering, University of Illinois, Urbana, IL 61801, USA.